

# MULTI-OBJECTIVE OPTIMIZATION OF STORAGE BATTERY OPERATION IN CLUSTERED RESIDENTIAL GRID-INTERCONNECTED PV

Contact person: Shinji WAKAO

Address: 3-4-1 Ohkubo, Shinjuku-ku, Tokyo 169-8555, JAPAN

Email: wakao@waseda.jp

Phone: +81-3-5286-3219, Fax: +81-3-3200-7993

Shingo KINOSHITA<sup>(1)</sup>, Takahiro SHIMOO<sup>(1)</sup>, Shinji WAKAO\*<sup>(1)</sup>, Yusuke MIYAMOTO<sup>(2)</sup>

(1) Waseda University, Tokyo, JAPAN

(2) Kandenko Co., Ltd., Ibaraki, JAPAN

**Abstract** – In the near future, photovoltaic (PV) power generation systems will become widespread. In this study, we apply multi-objective optimization to the designed model: the concentrated introduction of PV systems with stationary batteries and electric vehicle (EV) batteries in housing areas to fulfill the diverse demands from various sectors, including electrical power companies and utility customers. In the computations, we propose a novel method for modeling the residential load and PV output power based on the measured data from a national research project in Japan. Furthermore, we carry out data mining of the optimization results using a self-organizing map as an effective analysis tool for the design of PV systems with storage batteries.

**Keywords:** photovoltaic power generation, distribution network, stationary battery, electric vehicle, multi-objective optimization, self-organizing map

## 1 INTRODUCTION

Photovoltaic (PV) power generation is predicted to become one of most widespread measures to solve environmental and energy problems. Japan aims to increase the capacity of PV systems to 53 GW by 2030; residential grid-interconnected PV systems will account for 80 % of this target capacity.

When a number of PV systems are installed in a residential area, some technical problems are bound to occur. One of them is an increase in the grid voltage due to reverse power flow from the PV system. In this case, the PV output is reduced by a power conditioning system (PCS) to sustain the grid voltage (below 107 V in Japan). This phenomenon leads economic losses for PV installers.

To overcome the above problem, the application of stationary batteries and electric vehicles (EVs), which are expected to be extensively used as next-generation cars, is a possible energy buffer measure for reverse power flow. The coordination of stationary and EV batteries is very effective to provide various benefits to utility customers and electric power companies.

In this paper, given the above background, assuming the residential area model in which large quantities of PV systems are introduced, we have carried out the multi-objective optimization of the operation of stationary and EV batteries.

In the computations, we have also proposed a practical method for modeling the residential load and PV output power which are based on the measured data of the demonstrative research on clustered PV systems by New Energy and Industrial Technology Development Organization (NEDO) in Japan.

Furthermore, as the number of objective functions increases, it becomes difficult to appropriately evaluate the correlation among the objective functions and design variables. Therefore, we have attempted to effectively extract the design information of the PV system with batteries using self-organizing map (SOM) which is able to project multidimensional data into two dimensions. Some numerical examples, which show the effectiveness of the proposed methods, are also presented.

## 2 INVESTIGATED MODEL

### 2.1 Distribution network model

A residential area model, which consists of 18 residential clusters as shown in Fig. 1, is considered. Two clusters are connected to each point in the high-voltage network (P1 – P9). The distribution-line impedances are listed in Table. 1. PV systems are randomly introduced in 756 houses (66% of all houses).

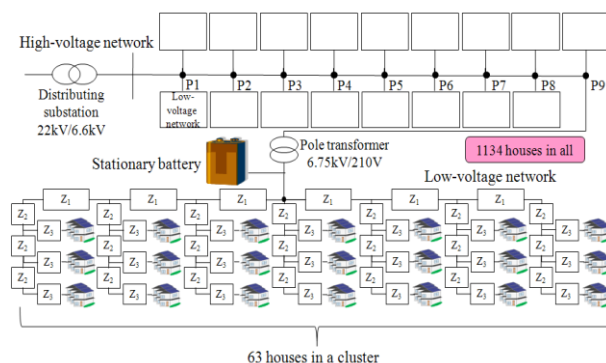


Figure 1: Distribution network model

High-voltage network	Impedance	0.313+j0.377 [ $\Omega$ /km]
Low-voltage network	Impedance $Z_1$	$3.73 \times 10^{-5} \Omega$ /m
	Impedance $Z_2$	$3.48 \times 10^{-4} \Omega$ /m
	Impedance $Z_3$	$8.90 \times 10^{-4} \Omega$ /m

Table 1: Distribution-line impedances

## 2.2 Stationary battery model

The characteristics of the stationary battery are listed in Table 2.

In the optimization procedure, the number of stationary batteries is varied. Since the grid voltage increases frequently at the terminal of the distribution network, stationary batteries are preferentially installed in clusters farther away from distributing substation. For example, in the case where the installation number is 4, the stationary batteries are set in the clusters connected to P8 and P9 in Fig. 1.

In the stationary battery operation, the amount of charged power corresponds to the surplus PV output over the threshold for charge; the amount of discharged power corresponds to the surplus load power over the threshold for discharge as shown in Fig. 2. Hence, the amount of discharged power is restricted so that no reverse power flow is generated by the stationary batteries. Taking into account the seasonality of load characteristics, the threshold for discharge is set in each season. As a result, the stationary battery operation is defined by the design variables listed in Table 3.

Type	Lead-acid
Rated DC voltage	192 V
Rated charging current	0.3 C [A]
Rated discharging current	0.4 C [A]
Depth of discharge	0 – 70 %
Charging voltage	211.2 V
Discharging voltage	187.2 V
Efficiency	89 %

**Table 2:** Characteristics of stationary battery

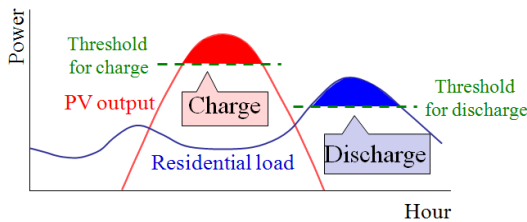


**Figure 2:** Conceptual figure of stationary and EV battery operation

Design variables	Range	Step size	Stationary battery	EV	
Threshold for charge	0 – 3.2 [kW]	0.05	Yes	Yes	
Threshold for discharge	spring	0 – 1.3 [kW]			0.05
	summer	0 – 1.3 [kW]			0.05
	autumn	0 – 1.3 [kW]			0.05
	winter	0 – 1.9 [kW]			0.05
Capacity	378 – 2058 [Ah]	42	No		
Number of batteries	2 – 18	2			

**Table 3:** Design variables of stationary and EV batteries

## 2.3 EV battery model and driving pattern

The characteristics of the EV battery, i.e., i-MiEV manufactured by Mitsubishi Motors, are listed in Table 4 [1] [2]. EVs are introduced in half of the houses with PV systems, i.e., 378 vehicles. We set three types of EV driving patterns as shown in Table 5 [3].

Capacity		16 kWh
Charge efficiency		90 %
Power consumption	spring , autumn	8.6 km/kWh
	summer	7.3 km/kWh
	winter	6.0 km/kWh

**Table 4:** Characteristics of EV battery

Pattern	Outgo [time]	Return [time]	Date of usage [days/week]	Running distance [km]	Number of vehicles
Commuting	7:00	20:00	5	24.5	162
Shopping	15:00	18:00	6	10	162
Leisure	7:00	20:00	1	95	54

**Table 5:** Driving patterns

## 2.4 Operation mode of EV battery

In order to examine the effectiveness of the application of EV batteries, three types of operation modes are set, as listed in Table 6.

MODE	Daytime charge of EV battery	V2H of EV battery
1	No	No
2	Yes	No
3	Yes	Yes

**Table 6:** Operation modes of EV battery

In mode 1, the EV battery is charged up to an SOC of 100% in the night, and the EV is driven on the following day. The battery is charged from 23:00 to 6:00, when power rates are low.

In mode 2, the EV battery is charged up to an SOC of 80% in the night only if the remaining charging capacity is insufficient to last through the next day's drive. In addition, the EV battery is charged in the daytime by using the PV output power in the same manner as that used to charge the stationary battery.

In mode 3, the nighttime charge and the daytime charge are the same as those in mode 2, and the EV battery is discharged for the residential load in the night, i.e., Vehicle to Home (V2H) in the same manner as that used to discharge the stationary battery.

Therefore, the operation of the EV battery system is defined by the design variables listed in Table 3.

## 2.5 Objective functions

Three types of objective functions, i.e., economic cost, CO<sub>2</sub> emission, and annual load factor, are investigated. The economic cost and CO<sub>2</sub> emission are aimed to be minimized; the annual load factor is aimed to be maximized.

### (i) Economic cost

The economic cost is one of the objective functions used for the evaluation of economic efficiency. It is the sum of the electric expenses of all the houses and the stationary battery costs. Electricity prices are listed in Table 7 [4]. The cost of the stationary battery is assumed to be 0.1765 USD/Ah (1 USD = 85 JPY), and its lifespan is set to be 10 years. The economic cost is expressed by (1).

$$\begin{aligned} \text{Economic cost [USD]} = & \text{expense of electric power purchase [USD]} \\ & - \text{income of electric power selling [USD]} \\ & + \text{stationary battery cost [USD]} \div 10 [\text{year}] \end{aligned} \quad (1)$$

Time zone	Price [USD / kWh] (1 USD = 85 JPY)
7:00~10:00, 17:00~23:00	0.2721
10:00~17:00	0.3327 (except summer), 0.3926 (summer)
23:00~7:00	0.1079
Selling	0.4471

Table 7: Electricity prices

### (ii) CO<sub>2</sub> emission

CO<sub>2</sub> emission is one of the objective functions for the evaluation of environmental load. The CO<sub>2</sub> emission coefficient of the power system is assumed to be 0.34kg-CO<sub>2</sub>/kWh [6]. The amount of CO<sub>2</sub> emitted during the manufacture of the stationary battery is assumed to be 2.20kg-CO<sub>2</sub> per battery weight of 1 kg on the basis of weight composition, amount of energy used, CO<sub>2</sub> basic unit, etc. [7]. CO<sub>2</sub> emission is expressed by (2).

$$\begin{aligned} \text{CO}_2 \text{ emission [ton]} = & \text{amount of CO}_2 \text{ emission by making battery [ton]} \\ & + \text{receiving electric power [kWh]} \\ & \times \text{CO}_2 \text{ emission coefficient [ton / kWh]} \end{aligned} \quad (2)$$

### (iii) Annual load factor

Annual load factor, an important index for electric power companies to ensure efficient power-supply, is one of the objective functions used for the evaluation of electric load leveling. The industrial load corresponding to the residential load in Fig. 1 is modeled, as shown in Fig 3 [8]-[10]. The annual load factor is defined by (3); the total load power is the sum of the residential and the industrial load. The details of the residential load are discussed in the next chapter.

$$\text{Annual load factor [\%]} = \frac{\text{average of total load power [kW]}}{\text{maximum of total load power [kW]}} \times 100 \quad (3)$$

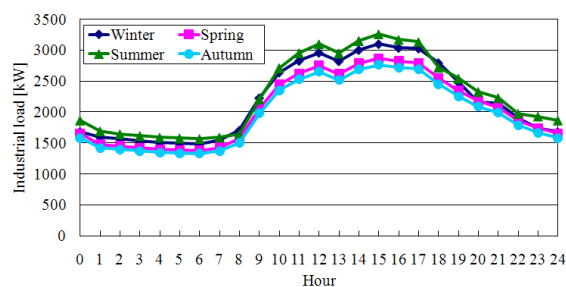


Figure 3: Industrial load model

## 2.6 Multi-objective optimization

In multi-objective optimization, Pareto optimal solutions are searched by using the multi-objective genetic algorithm (MOGA) [11]. Fig. 4 illustrates the concept of the Pareto optimal solutions for two objective functions ( $f_1$  and  $f_2$ ). The crosses on the edge of the search domain are Pareto optimal solutions. At this point, one objective function cannot be improved without deterioration of the other function. A designer finally selects

the most suitable solution from these solutions considering the various restriction conditions.

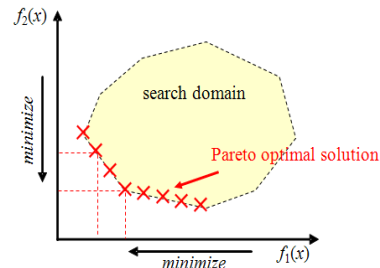


Figure 4: Conceptual figure of Pareto optimal solutions

## 3 MODELING METHOD OF RESIDENTIAL LOAD AND PV OUTPUT

In this study, two models of the residential load and PV output are investigated. In the simplified model, the unified residential load and PV output profiles are applied to all the houses. On the other hand, in the proposed model, the residential load and PV output profiles are different in each house. The proposed models are derived from the measured data of the demonstrative research on clustered PV systems conducted by NEDO in Japan. Therefore, the simulation results are more practical in the case of the proposed model. In this chapter, we compare the computational results of these models from a practical point of view.

### 3.1 Simplified model

The residential load profile in a simplified model is shown in Fig. 5; that is, this figure shows the profile of the power demand in an all-electric home [12]. The PV output profile is based on the solar radiation data of METPV [13].

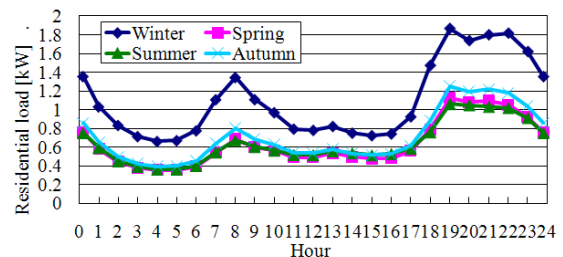


Figure 5: Residential load profile

### 3.2 Proposed model

In the proposed model, the residential load and the PV output data measured at 553 residences in the research project entitled “Demonstrative research on clustered PV systems by NEDO” are utilized [14].

The residential load profiles depend on the family configuration and lifestyle; the PV output profiles depend on the installation situations. Therefore, in order to classify the features of the residential load and PV output of 553 houses, we carry out clustering using the k-means++ method [15]. The adequate cluster number of the patterns of the residential load and PV output were determined to be 5. The ratio of the number of

members in each cluster to the total members is shown in Table 8. The averaged profiles of each cluster are shown in Fig. 7.



Figure 6: Demonstrative research on clustered PV systems

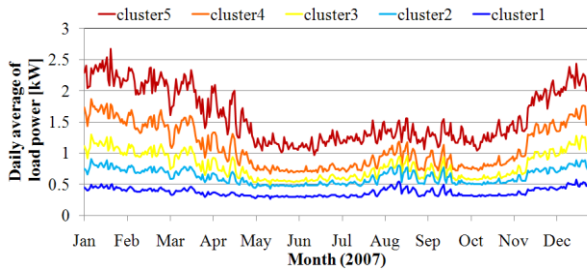
	Cluster 1	Cluster 2	Cluster 3	Cluster 4	Cluster 5
Ratio	13.6 %	42.9 %	24.1 %	17.0 %	2.5 %
Number	75	237	133	94	14

(a) Residential load

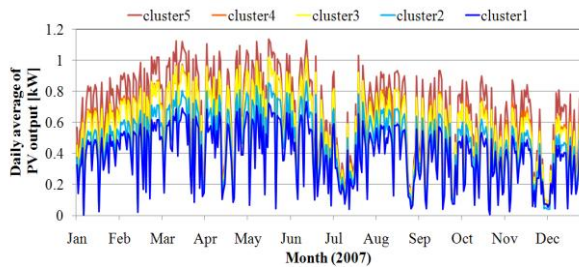
	Cluster 1	Cluster 2	Cluster 3	Cluster 4	Cluster 5
Ratio	23.3 %	22.8 %	15.7 %	18.6 %	19.5 %
Number	129	126	87	103	108

(b) PV output

Table 8: Ratio of number of members in each cluster to the total members



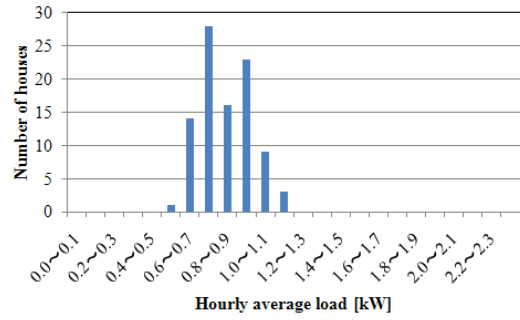
(a) Residential load



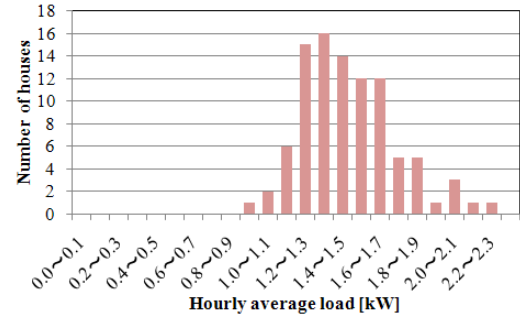
(b) PV output

Figure 7: Clustering results of load and PV output

Fig.8 shows the histograms of the hourly average residential load power of cluster 4 in spring and winter. It can be said that the variance depends on seasonality. Therefore, we have calculated the averages and standard deviations of the residential load and PV output of each cluster in each season. These averages and standard deviations are listed in Table 9. From Table 9 (a), we can see that the variance of the residential load increases in summer and winter when air conditioning is frequently used. On the other hand, from Table 9 (b), we can see that the variance of the PV output is larger in autumn and winter when the weather is changeable.



(a) Spring



(b) Winter

Figure 8: Histogram of hourly average load of cluster 4

Load	Spring		Summer		Autumn		Winter	
	Average [kW]	Standard deviation	Average [kW]	Standard deviation	Average [kW]	Standard deviation	Average [kW]	Standard deviation
Cluster 1	0.3156	0.0755	0.3702	0.0938	0.3914	0.1035	0.4135	0.1281
Cluster 2	0.5176	0.0856	0.5938	0.1135	0.6472	0.1053	0.7268	0.1364
Cluster 3	0.6251	0.0970	0.6998	0.1553	0.8376	0.1003	1.0131	0.1410
Cluster 4	0.8413	0.1340	0.8740	0.1970	1.1517	0.1740	1.4878	0.2501
Cluster 5	1.3118	0.1747	1.2877	0.2647	1.6542	0.1750	2.1229	0.4752

(a) Residential load

PV output	Spring		Summer		Autumn		Winter	
	Average [kW]	Standard deviation	Average [kW]	Standard deviation	Average [kW]	Standard deviation	Average [kW]	Standard deviation
Cluster 1	0.4710	0.0585	0.3609	0.0458	0.3035	0.0541	0.4494	0.0701
Cluster 2	0.5606	0.0529	0.4308	0.0429	0.3533	0.0489	0.5201	0.0614
Cluster 3	0.6636	0.0489	0.5044	0.0413	0.4276	0.0651	0.6284	0.0803
Cluster 4	0.6652	0.0434	0.5150	0.0322	0.4350	0.0466	0.6408	0.0594
Cluster 5	0.7542	0.0504	0.5853	0.0438	0.5190	0.0559	0.7555	0.0689

(b) PV output

Table 9: Average and standard deviation of each cluster

Assuming that the residential load and PV output are normally-distributed, we have designed a versatile model of the load and PV output by using the Box-Muller method [16]. We have modeled the residential load and PV output using the following expressions

$$\begin{cases} rLoad = \alpha \sqrt{-2 \ln(r_1)} \sin(2\pi r_2) + 1 \\ rPV = \alpha \sqrt{-2 \ln(r_1)} \sin(2\pi r_2) + 1 \end{cases} \quad (4)$$

$$\begin{cases} Load = rLoad \times Load\_ave \\ PV = rPV \times PV\_ave \end{cases} \quad (5)$$

where  $\alpha$  is a coefficient of variance of each cluster in each season.  $rLoad$  and  $rPV$  are numbers which follow normal distribution of average 1 and standard deviation  $\alpha$ .  $r_1$  and  $r_2$  are random numbers between 0 and 1.  $Load\_Ave$  and  $PV\_Ave$  denote the averaged profiles of

the residential load and PV output of each cluster, respectively, as shown in Fig. 7.

### 3.3 Verification of proposed models

In this section, the computational results of simplified and proposed models have been compared. The two-objective optimization in which the economic cost and the CO<sub>2</sub> emission are chosen as objective functions, was performed in mode 1 shown in Table. 6. The optimization results are shown in Fig. 9. The Pareto front of the proposed model is obviously different from that of the simplified model.

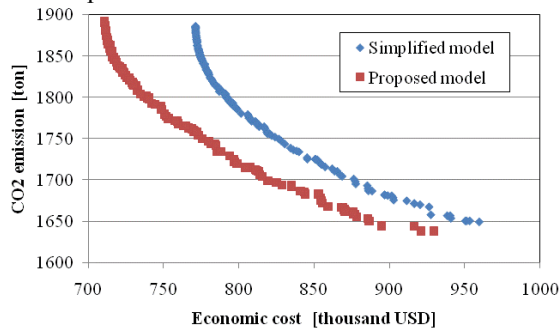


**Figure 9:** Results of two-objective optimization for 2 types of residential load and PV output models

Fig. 10 shows the average values of the residential load power in a day. Though the total electric demands of both models are equivalent, the fluctuation profiles of both models are different. In the proposed model, the averaged load power profile becomes smooth as compared to that of the simplified model because of the variance of the residential load power.

Consequently, by using the proposed modeling method, we can appropriately account for the smoothing effect in the residential load and PV output model, which results in a practical solution corresponding to actual conditions. Therefore, the following simulations are carried out using the proposed residential load and the PV output model.

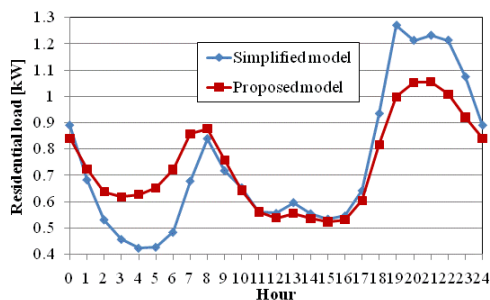


**Figure 10:** Average values of residential load in a day

## 4 COMPARISON AMONG OPERATION MODES OF EV BATTERIES

Two-objective optimization was carried out in 3 operation modes of the EV battery in Table 6 to clarify the effects of the daytime charge of the EV battery and V2H in the night. The optimization results are shown

in Fig. 11. The Pareto optimal solution of mode 3 is better than those of other modes. In mode 3, we can decrease the total capacity of stationary batteries because the EV batteries undertake the role of an energy buffer through daytime charge and V2H in the night. In other words, we can save the additional cost of stationary batteries in (1).

Therefore, we finally carry out three-objective optimization for the battery operation under the condition of mode 3, in the next chapter.

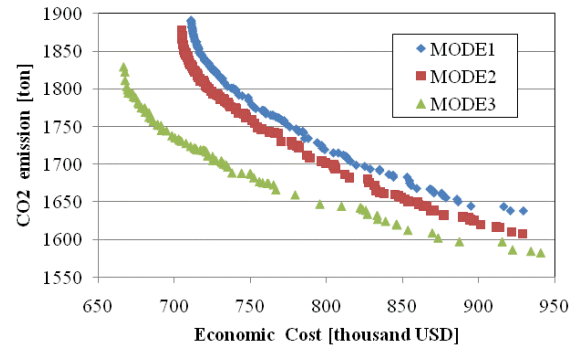


**Figure 11:** Results of two-objective optimization in 3 operation modes of EV battery

## 5 DATA MINING METHOD OF USEFUL DESIGN INFORMATION

In this chapter, three-objective optimization, with the added annual load factor, was carried out in mode 3, which is the best operation mode of the EV battery. Figs. 12 and 13 show the optimization results as graph on the 3 axes. The distribution of Pareto optimal solutions forms a planar and convex structure toward point O.

Analysis of correlation among objective functions and design variables is complicated because each Pareto solution has a number of components (15 components, i.e., 3 objective functions and 12 design variables). Thus, self-organizing map (SOM) is used to obtain the correlation.

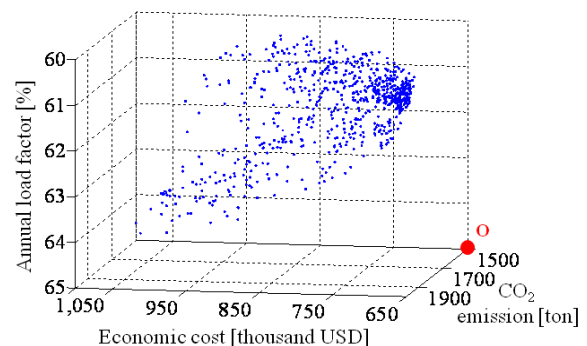


**Figure 12:** Results of three-objective optimization

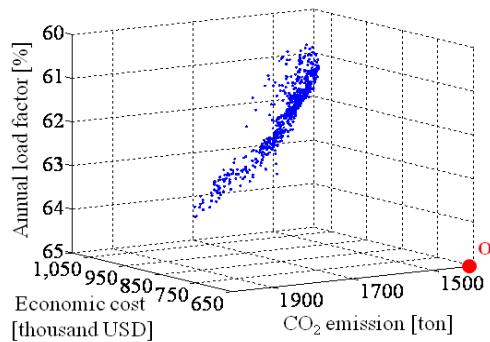


**Figure 13:** Results of three-objective optimization (different viewpoint from Fig.12)

### 5.1 Self-organizing map (SOM) [17]

SOM is a method to project multidimensional data in two dimensions. It enables us to visually understand the information contained in the data with ease because it explains the relationship of multi-dimensional data as the distance on a two-dimensional surface. Fig. 14 illustrates the concept of SOM.

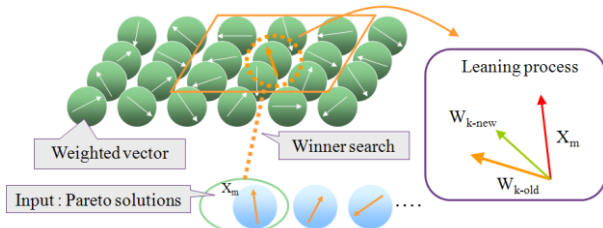


**Figure 14:** Conceptual figure of algorithm of SOM

Here, an example of analysis by SOM is provided. Three parameters have a relationship shown by the pink line in Fig. 15, and the blue lines are two-dimensional projections of the pink line. Line (a) obviously indicates the trade-off and nonlinear relationship between parameters 1 and 2. In addition, line (b) shows the nonlinear and positive correlation between parameters 1 and 3. Furthermore, the linear and negative correlation between parameters 2 and 3 can be read from line (c).

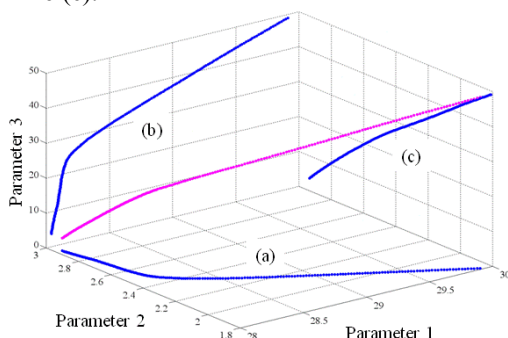
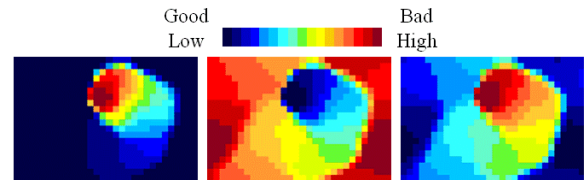


**Figure 15:** Example of 3 parameter relations

Fig. 16 shows the computational results of the application of SOM to the above example. Each figure corresponds to the map of each parameter, i.e., a component of data.



(a) Parameter 1 (b) Parameter 2 (c) Parameter 3

**Figure 16:** SOMs of 3 parameters

From Fig. 16, the strong negative correlation between parameters 2 and 3 is easily understood because the color of figure (b) is completely opposite to that of figure (c). This relationship corresponds to the result of line (c) in Fig. 15. Since the color of figure (a) is not identical but similar to that of figure (c), we can see that parameters 1 and 3 have positive and nonlinear correlation. In a similar way, a trade-off and nonlinear relationship between parameters 1 and 2 is understood.

Therefore, we can visually and easily extract the beneficial information for designing, such as the correlation among objective functions and design variables, through the proposed approach.

### 5.2 Analysis of three-objective optimization results by SOM

We applied the proposed method to the Pareto optimal solutions of three-objective optimization. 15 SOMs, 3 objective functions and 12 design variables, were drawn. 7 maps of the objective functions and design variables were selected from 15 maps, as shown in Fig. 17.  $\nabla$  and  $\triangle$  denote the minimum (good) and the maximum (bad) points in the SOMs, respectively.

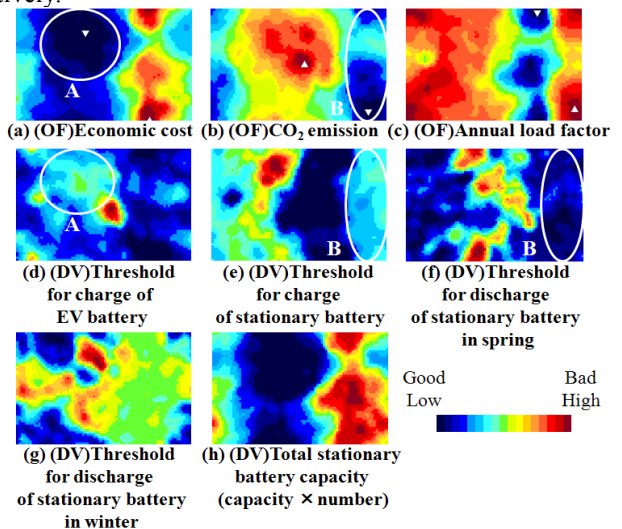


**Figure 17:** Analysis of three-objective optimization results

First, the relationships among objective functions were examined. Since the color pattern of figure (a) is opposite to that of figures (b) and (c), the economic cost is in almost negative correlation with the CO<sub>2</sub> emission and the annual load factor. Additionally, the CO<sub>2</sub> emission and annual load factor have nearly positive correlation.

lation with each other whereas there is a slight difference between the color patterns of figures (b) and (c).

Next, the relationship among each objective function and design variables is examined.

(i) Economic cost

The economic cost and the total stationary battery capacity are in strong correlation because figures (a) and (h) are very similar in color pattern.

In addition, focusing on circle A where the economic cost is very good, we find that the threshold for the charge of the EV battery should be set high to some extent. This indicates that reducing the amount of charged power supplied to the EV battery results in an increase of the reversal power flow from PV to grid, i.e., the increase in the income of the electric power selling.

(ii) CO<sub>2</sub> emissions

Figures (b) and (h) are obviously in negative correlation. Therefore, it is very effective to increase the total stationary battery capacity and charge a larger amount of PV output for reducing the electric power from the distribution network.

Additionally, focusing on circle B where the CO<sub>2</sub> emission is low, we find that the threshold for the charge of the stationary battery should be high to some extent and the threshold for its discharge of in spring should be low. This result indicates that we have to adequately set the threshold for the charge of the stationary battery in accordance with the surplus PV power; the stationary battery's capacity has to be secured for the charge of PV output in the next day, especially in spring when the amount of PV output is very large.

(iii) Annual load factor

In this optimization problem, the maximum total load power is obtained at around 18:00 in winter. Therefore, it is effective if the stationary battery discharges to the residential load at the above mentioned time for improving the annual load factor. Comparing figures (c) and (g), we can find that there is an adequate threshold value for the discharge of the stationary battery in winter, i.e., the green colored area in figure (g).

As seen above, the application of SOM makes it possible to efficiently extract the design information for improving the objective function values, which is useful in designing the PV systems.

## 6 CONCLUSIONS

In this study, the optimal operation of the stationary and EV batteries was investigated in a residential area where PV systems were introduced in large quantities. From the numerical results, the effectiveness of the cooperative operation of stationary and EV batteries has been presented.

In the computations, we proposed a novel method for modeling the residential load and PV output. The proposed method, based on the measured data from a na-

tional project in Japan, was also verified from the practical point of view.

Furthermore, the extraction of the system design information through the self-organizing map was also shown for efficiently improving the objective function values.

In the future work, we will investigate the stationary battery operation including the weather forecast and boost charge of EV batteries in a parking lot.

## REFERENCES

- [1] T. Hosokawa, K. Tanihara, and H. Miyamoto, "Development of I MiEV Next-Generation Electric Vehicle (Second Report)", Mitsubishi Motors Technical Review, No.20, pp 53-60, 2008 (In Japanese)
- [2] H. Koike, T. Hosokawa, K. Tanihara, S. Horie, and S. Irikata, "Joint On-Road Fleet Monitoring of "i-MiEV" New-Generation Electric Vehicle with Power Companies", Mitsubishi Motors Technical Review, No.21, pp 22-29, 2009 (In Japanese)
- [3] Japan Automobile Manufacturers Association Inc. website: <http://www.jama.or.jp/lib/jamareport/100/index.html> (In Japanese)
- [4] Tokyo Electric Power Company website: <http://www.tepco.co.jp/erates/individual/menu/home/home01-j.html> (In Japanese)
- [5] Ministry of Economy, Trade and Industry: <http://www.meti.go.jp/committee/materials2/downloadfiles/g80908a04j.pdf> (In Japanese)
- [6] Information Plaza of Electricity website: [http://www.fepe.or.jp/future/warming/taisaku/co2\\_mokuhyou/index.html](http://www.fepe.or.jp/future/warming/taisaku/co2_mokuhyou/index.html) (In Japanese)
- [7] K. Kajiyama, K. Okajima, and Y. Uchiyama, "Energy and Environmental Analysis of Batteries for Electric Load Leveling using LCA Method", Journal Life Cycle Assessment, Japan, Vol.2, No.4, pp 379-385, 2006 (In Japanese)
- [8] Federation of Electric Power Companies, "Graphical Filp-chart of Nuclear & Energy Related Topics 2011", Fig.1-22, 2011 (In Japanese)
- [9] Federation of Electric Power Companies, "Graphical Filp-chart of Nuclear & Energy Related Topics 2007", Fig.1-21, 2007 (In Japanese)
- [10] Ministry of Internal Affairs and Communications Statistics Bureau website: <http://www.stat.go.jp/data/kokusei/2005/kihon1/00/04.htm> (In Japanese)
- [11] C. M. Fonseca and P. J. Fleming, "Genetic Algorithms for Multiobjective Optimization: Formulation, Discussion and Generalization", Proceedings of the 5th ICGA, pp 416-423, 1993
- [12] NEDO Final Report, "Investigation and Study on Autonomy-Enhanced PV Power Generation System", 2006
- [13] A. Itagaki, H. Okamura, and M. Yamada, "Preparation of meteorological data set throughout Japan for suitable design of PV systems", WCPEC-3, Vol.2, pp 2074-2077, 2003
- [14] Y. Miyamoto and H. Sugihara, "Demonstrative research on clustered PV systems", 34th IEEE Photovoltaic Specialists Conference, 2009
- [15] D. Arthur and S. Vassilvitskii, "k-means++: the advantages of careful seeding", Proceedings of the eighteenth annual ACM-SIAM symposium on Discrete algorithms, pp 1027-1035, 2007
- [16] G.E.P. Box, and M.E. Muller, "A Note on the Generation of Random Normal Deviates" The Annals of Mathematical Statistics, No.2, pp 610-611, 1958
- [17] T. Kohonen, "Self-Organizing Maps", Springer-Verlag Tokyo, 2005 (In Japanese)
- [18] K. Sato and S. Wakao, "Operation design and data mining of battery system in photovoltaics", 24th European Photovoltaic Solar Energy Conf., Hamburg, Germany, pp 3882-3887, 2009
- [19] T. Shimoo, K. Sato, S. Wakao, and Y. Miyamoto "Operation design of PV system with storage battery in consideration of weather forecast information", 25th European Photovoltaic Solar Energy Conf., Valencia, Spain, pp 4859-4864, 2010